journal

J. Am. Ceram. Soc., 93 [9] 2530–2533 (2010)
DOI: 10.1111/j.1551-2916.2010.03878.x

Orientation and Phase Relationships between Titania Films and Polycrystalline $BaTiO_3$ Substrates as Determined by Electron Backscatter Diffraction Mapping

Nina V. Burbure, Paul A. Salvador, and Gregory S. Rohrer*,†

Department of Materials Science and Engineering, Carnegie Mellon University, Pittsburgh, Pennsylvania 15213-3890

Titania films have been grown on polycrystalline $BaTiO_3$ (BTO) substrates at 700°C by pulsed laser deposition. Electron backscatter diffraction (EBSD) was used to determine grain orientations in the substrate before growth, and the phase and orientation of the supported films after growth. All $BaTiO_3$ grains within 26° of (001) were covered by anatase films with an orientation relationship of $(001)_{Anatase}||(001)_{BTO}$ and $[100]_{Anatase}||[100]_{BTO}$. Rutile with a variety of orientations grew on $BaTiO_3$ grains with orientations closer to (110) and (111). EBSD mapping provides an efficient means for determining phase and orientation relationships of films over all orientation parameters.

I. Introduction

Thin titania films on $BaTiO_3$ (BTO) substrates are being investigated for potential photochemical applications.[1] The motivation is that the dipolar field from the ferroelectric substrate can influence the motion of photogenerated charge carriers in the catalytic titania overlayer and this effect, if adequately controlled, has the potential to limit charge carrier recombination. Because the phase and orientation are known to influence the photochemical reactivity of bulk titania,[2–6] they represent important factors in the design of a composite photocatalyst.

Prior research shows that titania films deposited on low-index, macroscopic, single-crystal perovskite surfaces (including $SrTiO_3$ and $LaAlO_3$, but not $BaTiO_3$) can form epitaxially as either anatase or rutile.[7–17] Experimentally, substrate orientation, lattice mismatch, temperature, and deposition rate influence the thermodynamics and kinetics of nucleation and growth in a way that controls the resulting film phase and orientation.[18–20] The most consistent observation in these reports, using different growth techniques and temperatures, is that anatase forms on (100) perovskite surfaces with an orientation relationship of $(001)_A||(100)_P$ and $[100]_A||[010]_P$, where A and P denote anatase and perovskite, respectively.[7–17] This is generally ascribed to the formation of a low-energy interface between the anatase and perovskite, owing to the nearly identical atom arrangement in anatase $TiO_2(001)$ and perovskite $ABO_3(100)$. When the mismatch between anatase ($a = 3.785$ Å, $c = 9.514$ Å) and the perovskite is increased from $LaAlO_3$ ($a = 3.778$ Å) to $SrTiO_3$ ($a = 3.905$ Å), films transition from single-phase anatase to a mixture of anatase and rutile (especially at higher temperatures or higher deposition rates).[15] The lattice mismatch between anatase and $BaTiO_3$ ($a = 4.012$ Å) is even larger.

The most consistent observation from growth studies on perovskites with orientations other than (100) is that rutile (R) forms on (111) perovskite surfaces with an orientation relationship of $(100)_R||(111)_P$ and $[001]_R||[1\text{–}10]_P$.[12,15] This result is rationalized in terms of the favorable lattice match between rutile(100) ($a = 4.5937$ Å, $c = 2.9581$ Å) and perovskite(111), which both have nearly hexagonal arrangements of oxygen with the shortest O–O distances being 2.779/2.958 Å in rutile(100) and 2.761 in $SrTiO_3$(111). The same distance in $BaTiO_3$ is about 2.837 Å, which provides a better average match. Two reports of the deposition of titania on (110) perovskite surfaces indicate that anatase forms with $(012)_A||(011)_P$ and $[010]_A||[100]_P$ and no reports exist on high-index planes present on polycrystalline substrates.[12,15]

The single previous study of orientation relationships between $BaTiO_3$ and TiO_2 was conducted by reacting $BaCO_3$ in the solid or gas form with (110) orientated rutile crystals between 700° and 900°C.[21] The orientation relationship depends on both the temperature and the reaction mechanism. In different cases, $BaTiO_3$ with (001), (110), (119), and (331) orientations grew on (110)-orientated rutile crystals. The fact that these results differ from similar experiments in which $SrTiO_3$ is reactively grown on the same substrate suggests that the orientation relationships determined for TiO_2 growth on $SrTiO_3$ and $LaAlO_3$ may not apply to TiO_2 to $BaTiO_3$.[16]

A common feature of the previous studies was that films were deposited on several low-index, macroscopic, single-crystal substrates and the orientation relationships were determined by X-ray diffraction (XRD). Here, a new approach is used. Instead of using many single crystals, whose availability frequently limits the scope of epitaxy studies, a polycrystalline substrate has been used. This substrate is a coarse-grained ceramic in which each grain can be thought of as a single crystal substrate with a different orientation. While these substrates are microscopic by comparison with conventional single crystals, they are large enough (>25 μm²) to be characterized by conventional electron probes and we therefore use electron backscatter diffraction (EBSD) in a scanning electron microscope (SEM) to determine the phase and orientation of titania films grown on a range of $BaTiO_3$ substrate orientations. The purpose of this paper is to identify the phase and orientation relationships for TiO_2 grown on $BaTiO_3$ at 700°C and to describe this new method for determining such relationships.

II. Experimental Methods

$BaTiO_3$ powder (Alfa Aesar, Ward Hill, MA; 99.7%) was ground and uniaxially compressed at 230 MPa to form cylinders with 11 mm diameters and 2–5 mm thicknesses. The samples were sintered in an alumina crucible containing excess $BaTiO_3$ powder to provide a barrier and minimize contamination from the crucible. The substrates were degassed for 10 h at 900°C, sintered for 10 h at 1230°C, and further annealed at 1360°C to yield grains of approximately 50 μm. A larger TiO_2

T. E. Mitchell—contributing editor

Manuscript No. 27717. Received March 19, 2010; approved April 17, 2010.
This work was supported by National Science foundation grants DMR 0412886 and DMR 0804770. Facilities supported by MRSEC program of the National Science Foundation under Award Number DMR-0520425 were used.
*Member, The American Ceramic Society.
†Author to whom correspondence should be addressed. e-mail: gr20@andrew.cmu.edu

target was similarly prepared, but with a final anneal of 1600°C for 24 h. To prepare the substrates for film growth, the samples were lapped flat using a 9 μm Al_2O_3 aqueous solution (Buehler, Lake Bluff, IL), polished with a 0.02 μm colloidal silica solution, and thermally etched in air for 4 h at 1200°C.

Titania films were grown using a PLD system (Neocera, Beltsville, MD) with a KrF laser ($\lambda = 248$ nm) operating at a frequency of 3 Hz and at an energy density of 2 J/cm^2. The distance between the target and the substrate was 6 cm. A base pressure of 10^{-6} torr was established before heating. Films were deposited at 700°C for approximately 90 min in a dynamic vacuum of 10 mtorr O_2. The films were cooled to room temperature in a static O_2 pressure of 5 torr. The film thickness, determined by X-ray reflectivity measurements of films on $SrTiO_3$ single crystals placed next to the sample during growth, was about 100 nm.

The orientations of specific substrate grains and supported films were determined by EBSD.[22] Backscatter patterns were acquired using a XL40FEG SEM (FEI, Hillsboro, OR) with the sample tilted at 70° and analyzed with TSL orientation imaging microscopy data collection and analysis software. In a typical experiment, the working distance was 10 mm, the spot size was 5 or 6, and the accelerating voltage of 20–30 kV. Patterns from the $BaTiO_3$ substrate were of high quality and orientation maps could be obtained automatically. Patterns from the film, on the other hand, were more diffuse, perhaps because of internal strain. Because the automated indexing produced results with a low confidence index, EBSD patterns from the film were indexed manually. In this process, simulated patterns based on the phases (rutile or anatase) and orientations suggested by the software were visually compared with the observed patterns to confirm the correct assignments. It should be noted that consistent patterns were found within each substrate grain and this indicates that each grain supports a single orientation.

All $BaTiO_3$ orientations are taken to be cubic; the c to a ratio for $BaTiO_3$ is so close to unity that it is difficult to measure by EBSD. Furthermore, $BaTiO_3$ is cubic at the growth temperature. The orientation assignment is expressed as a set of three Euler angles (ϕ_1,Φ, and ϕ_2) that describe the transformation of the sample reference frame to the local crystal reference frame.[23] This transformation can be expressed as a 3×3 orientation matrix, g

$$g(\phi_1, \Phi, \phi_2) = \begin{bmatrix} c\phi_1 c\phi_2 - s\phi_1 s\phi_2 c\Phi & s\phi_1 c\phi_2 + c\phi_1 s\phi_2 c\Phi & s\phi_2 s\Phi \\ -c\phi_1 s\phi_2 - s\phi_1 c\phi_2 c\Phi & -s\phi_1 s\phi_2 + c\phi_1 c\phi_2 c\Phi & c\phi_2 s\Phi \\ s\phi_1 s\Phi & -c\phi_1 s\Phi & c\Phi \end{bmatrix} \quad (1)$$

where s and c denote sine and cosine, respectively. The vector representing the surface normal in the sample reference frame is $n' = [001]$; the same vector in the crystal reference frame, n, is then given by

$$c_i g n' = n \quad (2)$$

In Eq. (2), c_i are the symmetry operators of the crystal system.[24] For the cubic substrate orientations, there are 24 proper symmetry operators, and therefore 24 equivalent vectors given by Eq. (2). Among these equivalents, we always select one in the same fundamental zone of orientation space. Here, it is the vector with three positive components such that $n_3 > n_2 > n_1$, where n_3, n_2, and n_1, are the components of n along the c, b, and a crystal axes, respectively. For the tetragonal films, there are only eight equivalent vectors and we select the one with three positive components and $n_2 > n_1$.

Knowing the two orientations, it is also possible to calculate the misorientation between the substrate and the film. The 3×3 matrix describing the misorientation (Δg) between the substrate and film is

$$\Delta g = c_i g_s (c_i g_f)^T \quad (3)$$

where c_i are the proper symmetry operators associated with the material with the lower symmetry (TiO_2) and g_s and g_f are the orientations of the film and substrate, respectively. Equation (3) produces $c_i^2 = 64$ equivalent representations of the misorientation. From Δg, it is possible to determine a direction common to the substrate and film (referred to as the misorientation axis) and an angle of rotation about that axis (the misorientation angle), which brings the lattice vectors of the crystals into coincidence.[25] We select the eight axis-angle combinations that fall in a fundamental zone of tetragonal orientation space used above. In this communication, we focus on the orientation relationship of the metastable anatase phase and the perovskite substrate.

III. Results

The orientations of the substrate grains are shown in Fig. 1(a). The data are divided up into five categories: points near (001) (marked by an x), near (111) (triangles), near (101) (circles), near (313) (squares), and those inclined from (001) (plus signs). Among the points marked by the plus signs, the furthest from (001) is inclined by 26°. The orientations of the films are shown in Fig. 1(b). Note that in this case, the orientations are represented in the larger fundamental zone for tetragonal materials and the figures are drawn so that, in both cases, the [001] direction points out of the page. The points on the left hand side correspond to anatase and the points on the right hand side correspond to rutile.

To illustrate the relationship between the substrate and film orientation, the same groups of data points are represented by the same symbols. By comparing Figs. 1(a) and (b), it can be seen that anatase grows on all of the substrate orientations inclined by $<26°$ from (001) and rutile grows on the others. Furthermore, the anatase that grows on (001)-oriented substrates

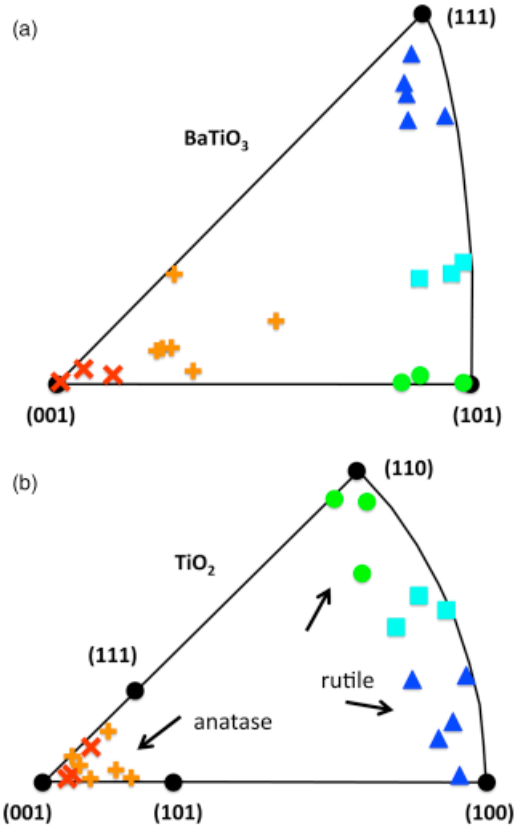

Fig. 1. Orientations of 20 (a) substrate grains and (b) supported films represented in a stereographic projection. The figure in (a) spans the domain of unique cubic orientation and (b) spans the domain of unique tetragonal orientations. Note that the markers for (111) and (101) apply only to rutile.

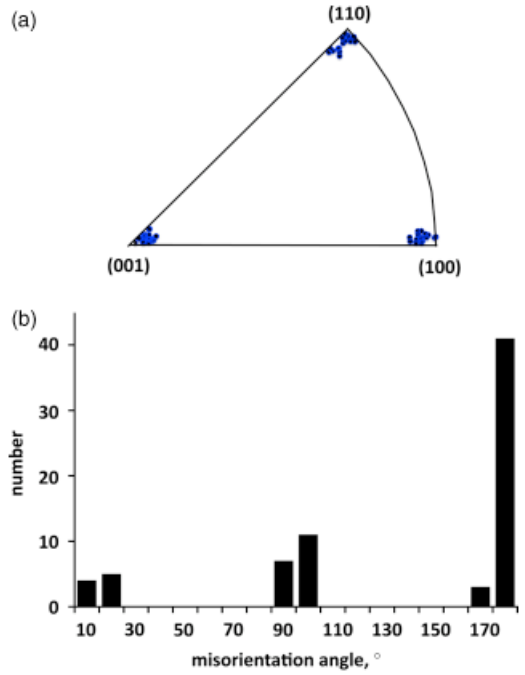

Fig. 2. The distributions of (a) misorientation axes and (b) misorientation angles for the anatase films. In Fig. 1, these are the orientation labeled by the "x" or the "+". (a) The orientation of each axis is indicated by a circle on a stereographic projection of the domain of unique tetragonal orientations. (b) Histogram showing the number of misorientation angles that fall into 10° bins.

also has the $(001)_A$ orientation. The rutile that grows on $BaTiO_3(111)$ has the $(100)_R$ orientation, that growing on $BaTiO_3(101)$ has the $(110)_R$ orientation, and that growing on $BaTiO_3(313)$ has the $(120)_R$ orientation.

The results on Fig. 1 show the relationship between the directions normal to the film (typically found for single crystal experiments by XRD), but do not provide information on the in-plane alignment of the lattices (found with XRD phi-scans or reciprocal space mapping). For this, we examine the calculated misorientations from the same EBSD patterns. Axis-angle pairs were determined for the nine substrate-film combinations where anatase grew. The distribution of misorientation axes is shown in Fig. 2(a). All of the misorientations can be described as rotations about [001], [010], or [110]. The distribution of misorientation angles, binned in 10° increments, is shown Fig. 2(b). Note that all of the angles are clustered around 0, $\pi/2$, or π. In the tetragonal system, rotations of 0, $\pi/2$, or π about [001], [010], or [110] bring the crystal to an indistinguishable orientation. Our interpretation is that the lattice vectors of both phases are aligned and the orientation relationship can be expressed as $(001)_A||(001)_S$ and $[100]_A||[100]_S$, identical to that observed for single crystal (100)-oriented perovskites.

IV. Discussion

The local phase and orientation relationships determined for TiO_2 on polycrystalline $BaTiO_3$ substrates are comparable with those established for TiO_2 on single-crystal $SrTiO_3$ and $LaAlO_3$,[7–17] and this provides confidence in this EBSD-based technique. Specifically, (001) anatase grows on (001) $BaTiO_3$ and (100) rutile grows on (111) $BaTiO_3$. These observations indicate that the larger lattice mismatch of $BaTiO_3$ with anatase does not necessarily change the growth of the epitaxially stabilized film under these growth conditions.

One interesting aspect of the current findings is the wide range of stability of the $(001)_A||(001)_{BTO}$ and $[100]_A||[100]_{BTO}$ orientation relationship. Even when the substrate is misoriented by as much as 26°, the crystal axes of anatase and $BaTiO_3$ remain aligned. This means that for heteroepitaxial films grown on planar substrates, it is possible to prepare metastable anatase films with a wide range of high index orientations in the neighborhood of [001]. This suggests that the film–substrate interface has a particularly strong influence on anatase growth in these kinetic conditions, overwhelming the increase in surface energy. It is possible that the stability of the orientation relationship is aided by microscopic surface faceting, resulting in a decrease in the surface energy term. It has been reported that anatase films with the (102) orientation microfacet to reveal lower energy (101) surfaces.[13] It may be that orientations in the neighborhood of (001) are terminated by similar microfaceted surfaces that offset the increase in the film-substrate energy arising from in-plane mismatches.

The observation that rutile(110) grows on $BaTiO_3(110)$ grains differs in some respects to earlier findings, although they are not completely inconsistent. For example, while anatase(102) was observed to grow on $SrTiO_3(110)$ crystals at lower temperatures, rutile was reported grow at 800°C.[15] Anatase in this orientation also grows on $LaAlO_3(110)$, even up to 900°C.[15] Two differences between these two studies are the growth procedures and the larger lattice mismatch of anatase and $BaTiO_3$. In Lotnyk *et al.*[15] electron beam evaporation was used with a continual growth rate of 0.1 Å/s. Our average growth rate was about 0.19 Å/s and the instantaneous growth rate was higher owing to the pulsed supply of material. For $SrTiO_3(110)$ and $BaTiO_3(110)$, where the preference for metastable anatase is reduced, an increase in temperature and growth rate will favor the stable phase. Further evidence that the observed orientation relationship is plausible is provided by the observation that when $SrTiO_3$ grows on rutile(110), it grows in the (110) orientation and when $BaTiO_3$ grows on rutile(110), one of the possible orientations it can take is (110).[16,21] The fact that the latter is reported to be mechanism dependent indicates that subtle variations in kinetics can alter the observed growth outcomes.

The use of EBSD to determine orientation relationships for thin films offers a number of advantages, although it also has limitations. The main advantage is that it makes it possible to explore a wide range of substrate orientations in a single experiment. The second advantage is that it makes it possible to study epitaxy in cases where single crystals are not available and, in nonperovskite systems, this is common. For example, there are many complex layered phases that have interesting properties and require novel approaches for understanding phase formation.[26,27] One disadvantage, with respect to XRD, is angular resolution. Absolute orientation measurements by conventional EBSD typically have errors of several degrees. Also, because the sample must be removed from the SEM for film growth and then remounted in the microscope, there will be a small misorientation that results from the imperfect alignment of the sample. Because the quality of the diffraction patterns from the films makes automatic indexing a challenge, it was not possible to take full advantage of the automated features in the OIM analysis software. This will presumably be sample dependent. However, a significant advantage with respect to XRD is that local orientation is determined. This makes it possible to check for structural uniformity and to identify specific regions that could be removed by ion beam milling and studied more carefully by transmission electron microscopy.

V. Conclusion

At 700°C, anatase and rutile grow simultaneously on $BaTiO_3$, depending on the substrate orientation. For growth on $BaTiO_3$ within 26° of the (001) orientation, epitaxially stabilized anatase grows with the orientation relationship of $(001)_A||(001)_{BTO}$ and $[100]_A||[100]_{BTO}$. Near $BaTiO_3(111)$, rutile grows in the (100) orientation and near $BaTiO_3(101)$, rutile grows with the (110) orientation. EBSD mapping of polycrystalline substrates provides an efficient means for determining phase and orientation

relationships and opens the door for investigating a range of materials for which it was difficult or impossible previously.

References

[1]N. V. Burbure, P. A. Salvador, and G. S. Rohrer, "Influence of Dipolar Fields on the Photochemical Reactivity of Thin Titania Films on $BaTiO_3$ Substrates," *J. Am. Ceram. Soc.*, **89** [9] 2943–5 (2006).

[2]L. Kavan, M. Gratzel, S. E. Gilbert, C. Klemenz, and H. J. Scheel, "Electrochemical and Photoelectrochemical Investigation of Single-Crystal Anatase," *J. Am. Chem. Soc.*, **118** [28] 6716–23 (1996).

[3]P. A. Morris Hotsenpiller, J. D. Bolt, W. E. Farneth, J. B. Lowekamp, and G. S. Rohrer, "The Orientation Dependence of Photochemical Reactions on TiO_2 Surfaces," *J. Phys. Chem. B*, **102** [17] 3216–26 (1998).

[4]J. B. Lowekamp, G. S. Rohrer, P. A. Morris Hotsenpiller, J. D. Bolt, and W. E. Farneth, "The Anisotropic Photochemical Reactivity of Bulk TiO_2 Crystals," *J. Phys. Chem. B*, **102** [38] 7323–7 (1998).

[5]T. Ohno, K. Sarukawa, and M. Matsumura, "Crystal Faces of Rutile and Anatase TiO_2 Particles and their Roles in Photocatalytic Reactions," *New J. Chem.*, **26** [9] 1167–70 (2002).

[6]T. Taguchi, Y. Saito, K. Sarukawa, T. Ohno, and M. Matsumura, "Formation of New Crystal Faces on TiO_2 Particles by Treatment with Aqueous HF Solution or Hot Sulfuric Acid," *New J. Chem.*, **27** [9] 1304–6 (2003).

[7]S. Chen, M. G. Mason, H. J. Gysling, G. R. Paz-Pujalt, T. N. Blanton, T. Castro, K. M. Chen, C. P. Fictorie, W. L. Gladfelter, A. Franciosi, P. I. Cohen, and J. F. Evans, "Ultrahigh Vacuum Metalorganic Chemical Vapor Deposition Growth and In Situ Characterization of Epitaxial TiO_2 Films," *J. Vac. Sci. Technol. A*, **11** [5] 2419–29 (1993).

[8]W. Sugimura, A. Yamazaki, H. Shigetani, J. Tanaka, and T. Mitsuhashi, "Anatase-Type TiO_2 Thin Films Produced by Lattice Deformation," *Jpn. J. Appl. Phys.*, **36** [12A] 7358–9 (1997).

[9]G. S. Herman and Y. Gao, "Growth of Epitaxial Anatase (001) and (101) Films," *Thin Solid Films*, **397** [1–2] 157–61 (2001).

[10]S. Yamamoto, T. Sumita, T. Yamaki, A. Miyashita, and H. Naramoto, "Characterization of Epitaxial TiO_2 Films Prepared by Pulsed Laser Deposition," *J. Cryst. Growth*, **237–239** [1] 569–73 (2002).

[11]C. C. Hsieh, K. H. Wu, J. Y. Juang, T. M. Uen, J.-Y. Lin, and Y. S. Gou, "Monophasic TiO_2 Films Deposited on $SrTiO_3$(100) by Pulsed Laser Ablation," *J. Appl. Phys.*, **92** [5] 2518–23 (2002).

[12]R. J. Kennedy and P. A. Stampe, "The Influence of Lattice Mismatch and Film Thickness on the Growth of TiO_2 on $LaAlO_3$ and $SrTiO_3$ Substrates," *J. Cryst. Growth*, **252** [1–3] 333–42 (2003).

[13]W. Gao, R. Klie, and E. I. Altman, "Growth of Anatase Films on Vicinal and Flat $LaAlO_3$ (110) Substrates by Oxygen Plasma Assisted Molecular Beam Epitaxy," *Thin Solid Films*, **485** [1–2] 115–25 (2005).

[14]P. Fisher, O. Maksimov, H. Du, V. D. Heydemann, M. Skowronski, and P. Salvador, "Growth, Structure, and Morphology of TiO_2 Films Deposited by Molecular Beam Epitaxy in Pure Ozone Ambients," *Microelectron. J.*, **37** [12] 1493–7 (2006).

[15]A. Lotnyk, S. Senz, and D. Hesse, "Epitaxial Growth of TiO_2 Thin Films on $SrTiO_3$, $LaAlO_3$ and Yttria-Stabilized Zirconia Substrates by Electron Beam Evaporation," *Thin Solid Films*, **515** [7–8] 3439–47 (2007).

[16]A. Lotnyk, S. Senz, and D. Hesse, "Orientation Relationships of $SrTiO_3$ and $MgTiO_3$ Thin Films Grown by Vapor-Solid Reactions on (100) and (110) TiO_2 (Rutile) Single Crystals," *J. Phys. Chem. C*, **111** [17] 6372–9 (2007).

[17]X. Weng, P. Fisher, M. Skowronski, P. A. Salvador, and O. Maksimov, "Structural Characterization of TiO_2 Films Grown on $LaAlO_3$ and $SrTiO_3$ Substrates Using Reactive Molecular Beam Epitaxy," *J. Cryst. Growth*, **310** [3] 545–50 (2008).

[18]M. Ohring, *The Materials Science of Thin Films*, 1st edition, Academic Press, New York, 2001.

[19]J. A. Venables, G. D. T. Spiller, and M. Hanbucken, "Nucleation and Growth of Thin Films," *Rep. Prog. Phys.*, **47** [4] 399–459 (1984).

[20]R. F. C. Farrow, "The Stabilization of Metastable Phases by Epitaxy," *J. Vac. Sci. Technol. B*, **1** [2] 222–8 (1983).

[21]A. Lotnyk, S. Senz, and D. Hesse, "Formation of $BaTiO_3$ Thin Films from (110) TiO_2 Rutile Single Crystals and $BaCO_3$ by Solid State Reactions," *Solid State Ionics*, **177** [5–6] 429–36 (2006).

[22]B. L. Adams, S. I. Wright, and K. Kunze, "Orientation Imaging—The Emergence of a New Microscopy," *Met. Trans. A*, **24** [4] 819–31 (1993).

[23]H.-J. Bunge, *Texture Analysis in Materials Science*. Butterworths, London, U.K., 1982, p. 21 (Translated by P.R Morris).

[24]U. F. Kocks, C. N. Tome, and H.-R. Wenk, *Texture and Anisotropy*. Cambridge University Press, Cambridge, U.K., 2000, p. 25.

[25]J. Pospiech and K Lucke, "The Rolling Textures of Copper and α-Brasses Discussed in Terms of the Orientation Distribution Function," *Acta Metall.*, **23** [8] 997–1007 (1975).

[26]S. Havelia, S. Wang, K. R. Balasubramaniam, and P. A. Salvador, "Thin Film Synthesis and Structural Characterization of a New Kinetically Preferred Polymorph in the $RE_2Ti_2O_7$ (RE = La–Y) Family," *Cryst. Growth Des.*, **9** [10] 4546–54 (2009).

[27]K. R. Balasubramaniam, S. Havelia, P. A. Salvador, H. Zheng, and J. F. Mitchell, "Epitaxial Stabilization and Structural Properties of $REMnO_3$ (RE = Dy,Gd,Sm) Compounds in a Layered, Hexagonal ABO_3 Structure," *Appl. Phys. Lett.*, **91** [23] 232901 (2007). □